JOURNAL OF SOLID STATE CHEMISTRY 29, 401–415 (1979)

Trends in Heavy-Metal Solid State Ionic Conductors: A Comparison of Cu^+, Ag^+, In^+, and Tl^+ Transport

R. L. AMMLUNG, RAYMOND P. SCARINGE, JAMES A. IBERS,* AND D. F. SHRIVER*

Department of Chemistry and Materials Research Center, Northwestern University, Evanston, Illinois 60201

AND D. H. WHITMORE

Materials Science Department and Materials Research Center, Northwestern University, Evanston, Illinois 60201

Received November 17, 1978

The mobility of Cu^+, Ag^+, In^+, and Tl^+ in halide compounds has been investigated to develop an understanding of the factors which are important in fast ion conduction. Many of the compounds in the comparison are of the type $MM'X_4$, where M is one of the monopositive ions listed above, M' is Zn^{2+}, Cd^{2+}, or Hg^{2+}, and X is Br^- or I^-. These compounds are characterized by transitions at elevated temperatures to disordered phases in which the M ion is highly mobile. Trends in the transition temperatures, conductivities, and activation energies for ion transport demonstrate that In^+ and Tl^+ are less mobile than Cu^+ and Ag^+. The crystal structure of the low-temperature phase of Tl_2ZnI_4 has been determined at −160°C. The material crystallizes with two formula units in space group C_2^2-$P2_1$ of the monoclinic system in a cell of dimensions $a = 7.661\ (9)$ Å, $b = 7.971\ (8)$ Å, $c = 10.074\ (13)$ Å, $\beta = 118.39\ (4)°$. The Zn^{2+} ions are tetrahedrally coordinated by I^- ions. The Tl^+ ions are found to reside in seven-coordinate sites approximating C_{2v} capped trigonal prisms. There is no clear-cut migration path for the Tl^+ ions, but some plausible conduction mechanisms are discussed. The origin of the mobility difference between d^{10} ions (e.g., Cu^+ and Ag^+) and $d^{10}s^2$ ions (e.g., In^+ and Tl^+) is attributed to the symmetry of the polarized ion. Compounds synthesized for the first time in the present work are In_2ZnBr_4 and Tl_2ZnBr_4. Materials which were discovered to be fast ion conductors are Ag_2ZnI_4, Ag_2CdBr_4, and Tl_2ZnBr_4.

Introduction

Certain ionic crystals are known to display ionic conductivity as high as the best liquid electrolytes. In the early 20th century Tublandt and Lorenz found that silver iodide, AgI, has a highly conducting phase which is stable between 147 and 550°C, with silver ion being the conducting species (*1*). Since then, a variety of solid state fast ion conductors have been discovered. Some of these may be described as framework materials having a rigid network through which the ions move. For example, the β-aluminas consist of conducting planes separated by alumina spinel slabs. A wide variety of monopositive ions, including the alkali metal ions, Tl^+, and Ag^+, can be ion exchanged for Na^+; however, Na^+ and Ag^+ have the highest mobilities (*2*). Another class of ionic conductors is based on heavy-metal halides for which the halide array is highly compliant. The two simplest examples in this

* Addressees for correspondence.

0022-4596/79/090401-15$02.00/0
Copyright © 1979 by Academic Press, Inc.
All rights of reproduction in any form reserved.
Printed in Great Britain

class are AgI and CuI (*3*). Compounds with more complicated compositions also fall into this second class. Examples include Ag_2HgI_4 (*4*) and Cu_2HgI_4 (*5*), MAg_4I_5 (M = Rb, K, or NH_4) (*6*, *7*), and compounds with partial substitution of silver or copper ions by organic ammonium ions (*8*).

The heavy-metal fast ion conductors, such as AgI, share several common properties. Structurally, these materials consist of a disordered arrangement of mobile cations within a relatively immoble anion array. With some compounds, such as $RbAg_4I_5$, this disordered phase is stable at room temperature, whereas with most others this phase becomes stable at higher temperatures.

The conductivities of these compounds in their disordered phases range from 1.0×10^{-3} $(\text{ohm-cm})^{-1}$ for Ag_2HgI_4 at 60°C (*4*) to 1.0 $(\text{ohm-cm})^{-1}$ for AgI at 150° (*1*). The highest solid state ionic conductivity reported at room temperature is 0.27 $(\text{ohm-cm})^{-1}$ for $RbAg_4I_5$ (*9*). Generally, the total conductivity of one of these disordered compounds is 10^2 to 10^3 greater than the conductivity of the ordered phases. The activation energies for ionic conduction in these compounds are very low, ranging from 5 kJ mole^{-1} for α-AgI (*10*) to 36 kJ mole^{-1} for Ag_2HgI_4 (*4*) and 60 kJ mole^{-1} for Cu_2HgI_4 (*5*).

Armstrong, Bulmer, and Dickinson have compiled a list of empirical generalizations for heavy-metal ionic conductors (*11*): the cation should be monovalent; the cation should be stable in environments of low coordination number; and the cation and anion should both be very polarizable. The influence of cation polarizability has been nicely demonstrated by Sleight, Gulley, and Berzins (*12*), who found that highly polarizable cations are much more mobile than less polarizable ions in isostructural compounds of the general formula $A^{1+}M_2X_6$ (where the mobile ion A^+ is Rb^+, Cs^+, or Tl^+; M is Ta, Nb, or W; and X is O or F). Thus, despite the fact that Tl^+ and Rb^+ are essentially the same size, Tl^+ has a much higher mobility in a given $M_2X_6^-$ framework.

The work summarized here was designed to test the influence of electronic structure on the mobility of monopositive heavy-metal ions, through a comparative study of d^{10} ions (Cu^+ and Ag^+) with $d^{10}s^2$ ions (In^+ and Tl^+). The monopositive indium ion is slightly larger than the silver ion [r = 1.27 Å for Ag^+ (*13*), r = 1.32 Å for In^+ (*14*)] and periodic trends suggest higher polarizability for In^+ than for Ag^+. This ion also is known in environments of low coordination number (*15*, *16*). The thallium(I) ion has a radius of 1.54 Å and its chemistry resembles that of the silver(I) ion (*13*). In order to make useful comparisons many different potential In and Tl ionic conductors were prepared, the more promising materials were physically and chemically characterized, and an X-ray structure determination was performed on a representative Group III conductor, Tl_2ZnI_4.

Results and Discussion

Preparation and Characterization

In previous work we reported that In_2ZnI_4, Tl_2ZnI_4, and In_4CdI_6 exhibit appreciable solid state ionic conductivity (*17*). However, these compounds undergo transitions into the disordered conducting phases at temperatures above 200°C, much higher than the best silver and copper ion conductors. In addition, the ionic conductivities are relatively poor in the disordered phases: 1.5×10^{-4} $(\text{ohm-cm})^{-1}$ for In_2ZnI_4 at 220°C, and 1.5×10^{-4} $(\text{ohm-cm})^{-1}$ for Tl_2ZnI_4 at 260°C. The ionic conductivity is greater than the electronic conductivity in the disordered phase by less than a factor of 100. In more recent work attempts have been made to extend the series of In^+ and Tl^+ conductors and thereby provide a firmer basis for the comparison with Cu^+ and Ag^+

conductors. One class of compounds which was investigated is A_2MX_4, where A is Ag, Cu, Ga, In, or Tl; M is Zn or Cd; and X is Br or I. Attempts also were made to prepare compounds of indium(I) and thallium(I) iodide where the metal ion is partially substituted by an organic ammonium ion. The products of these preparations have been characterized by elemental analysis, differential thermal analysis (DTA), powder X-ray diffraction, and variable temperature Raman spectroscopy. Variable temperature Raman spectroscopy is sensitive to the onset of disorder in heavy-metal halides and therefore is a useful tool for screening potential ionic conductors (*18*). Conductivity measurements were made using both reversible and ion blocking electrodes to determine the magnitude of the conductivity and identity of the charge carrier.

The reactions of indium(I) bromide with zinc bromide and cadmium bromide failed to produce compounds of appreciable conductivity. A new pale yellow compound having the composition In_2ZnBr_4 displays a unique X-ray powder pattern and a congruent melting point (215°C). The observation of a peak at 175 cm^{-1} in the Raman spectrum indicates the presence of the $ZnBr_4^{2-}$ species (*19*). The Raman spectrum of this compound remains essentially unchanged up to the melting point, indicating that no disordering occurs. Similarly, there is no evidence for a polymorphic phase transition from DTA, and the conductivity is low (1.2×10^{-7} (ohm-cm)$^{-1}$ 25°C) and totally electronic in nature up to the melting point. The orange material of the composition In_2CdBr_4 appears to be a mixture. For example, the Raman spectrum indicates the presence of InBr, $CdBr_2$ (*20*), and $CdBr_4^{2-}$ (*21*) and the X-ray powder pattern consists of some unidentified lines as well as lines attributable to InBr and $CdBr_2$. There is no evidence for the onset of disorder in this material and the conductivity is low (1×10^{-10} (ohm-cm)$^{-1}$ at 25°C) and totally electronic to 220°C, the melting point of InBr. No further attempt was made to prepare a pure phase.

Two new congruently melting compounds, Tl_2ZnBr_4 and Tl_2CdBr_4, have been prepared from the appropriate metal bromides and characterized. The colorless compound Tl_2ZnBr_4 melts at 330°C and undergoes a polymorphic phase transition at 215°C. This compound belongs to the monoclinic crystal system, and apparently is isomorphous with Tl_2ZnI_4 (vide infra). The Raman spectrum at 25°C indicates the presence of the $ZnBr_4^{2-}$ tetrahedral species (*23*). Upon heating the compound above 215°C its spectrum shows dramatic line broadening in the region below 100 cm^{-1}, an observation consistent with a disordered structure (Fig. 1). The conductivity of this compound is relatively low and mainly electronic at 25°C (1×10^{-9} (ohm-cm)$^{-1}$) but at 215° it jumps to 3×10^{-6} (ohm-cm)$^{-1}$. At this temperature the electronic conductivity is 3×10^{-7} (ohm-cm)$^{-1}$, indicating that there is a considerable electronic component to the total conductivity above 215°C. The colorless compound, Tl_2CdBr_4, which has been previously reported (*22*), displays a single DTA exotherm at 325°C and the X-ray powder pattern is unique. However, the strong peaks at 164 and 144 cm^{-1} in the Raman spectrum suggests the presence of both a $CdBr_4$ tetrahedron (*21*) and a $CdBr_6$ octahedron (*20*). As the sample is heated, these Raman peaks broaden slightly, as do other low-frequency peaks, but there is no dramatic change, indicating that no disordering occurs. The conductivity is low, 1×10^{-9} (ohm-cm)$^{-1}$ at 50°C, and apparently electronic to the melting point.

The previously reported incongruently melting compounds Ag_2ZnI_4 (*23*) and Ag_2CdI_4 (*24*) have been prepared by sintering below the peritectic point. Differential thermal analysis of Ag_2ZnI_4 reveals exotherms consistent with the published phase diagram. This compound undergoes a phase transition at 145°C and melts incongruently

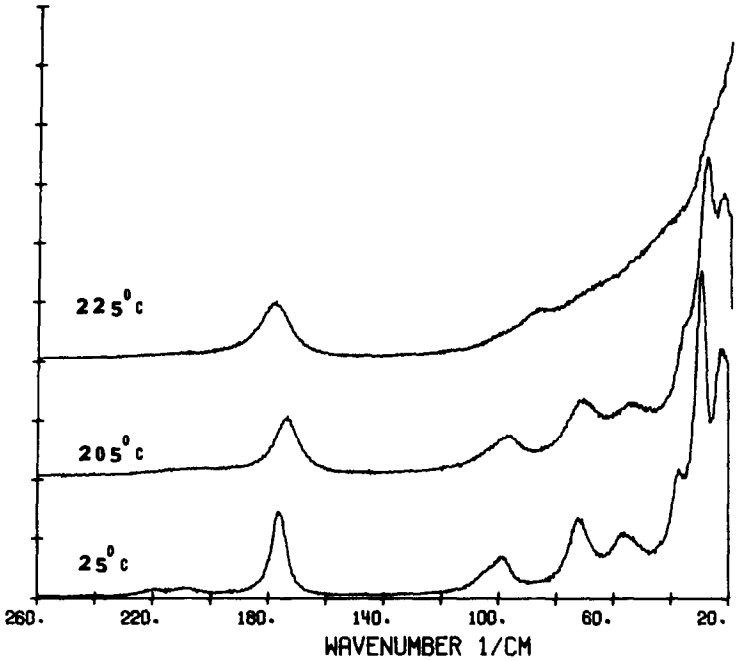

FIG. 1. Variable temperature Raman spectra of Tl_2ZnBr_4.

at 206°C. The Raman spectrum at 25°C consists of a strong, sharp peak at 127 cm^{-1} from ZnI_4^{2-} (*19*) and a broad peak at 98 cm^{-1} which is assigned to Ag–I stretching vibrations by analogy to Ag_2HgI_4 (*25*). These and other low-frequency peaks broaden above 145°C, suggesting the onset of disorder (Fig. 2). At 145°C the total conductivity increases by a factor of roughly 500 to 5×10^{-3} at 150°C. Ion blocking electrodes yield a conductivity of 1×10^{-5} (ohm-cm)$^{-1}$ at 150°C, demonstrating that the conductivity is largely ionic in the high-temperature phase. The room temperature conductivity is low, 5×10^{-8} (ohm-cm)$^{-1}$ at 25°C, and electronic in nature.

The X-ray powder pattern of Ag_2CdI_4 is consistent with the reported β-phase, which belongs to the hexagonal crystal system. Thermal analysis shows a weak exotherm at 80°C followed by a stronger exotherm at 130°C. The first may result from a phase transition to the reported α-phase, whereas the second exotherm is apparently a manifestation of decomposition. Higher-temperature exotherms are consistent with literature reports. The Raman spectrum consists of a strong peak at 121 cm^{-1} from CdI_4^{2-} (*21*) and some weak, broad peaks around 80 and 100 cm^{-1} from Ag–I vibrations. The spectrum loses intensity and broadens above 80°C, suggesting disorder (Fig. 3). The conductivity measured using reversible electrodes increases by a factor of 10^3 at 80°C to a value of 7×10^{-3} (ohm-cm)$^{-1}$. The electronic conductivity at this temperature, measured using blocking electrodes, is 1×10^{-5} (ohm-cm)$^{-1}$. Thus, the conductivity is mainly ionic in the high-temperature phase and electronic in the low-temperature phase.

Attempts to prepare compounds from a cadmium or zinc halide with silver bromide, copper bromides, or copper iodide resulted in the formation of solid solutions. In the case of the copper halides this is not surprising since Herrmann reported in 1911 that the CuI–CdI_2 and CuBr–$CdBr_2$ systems form

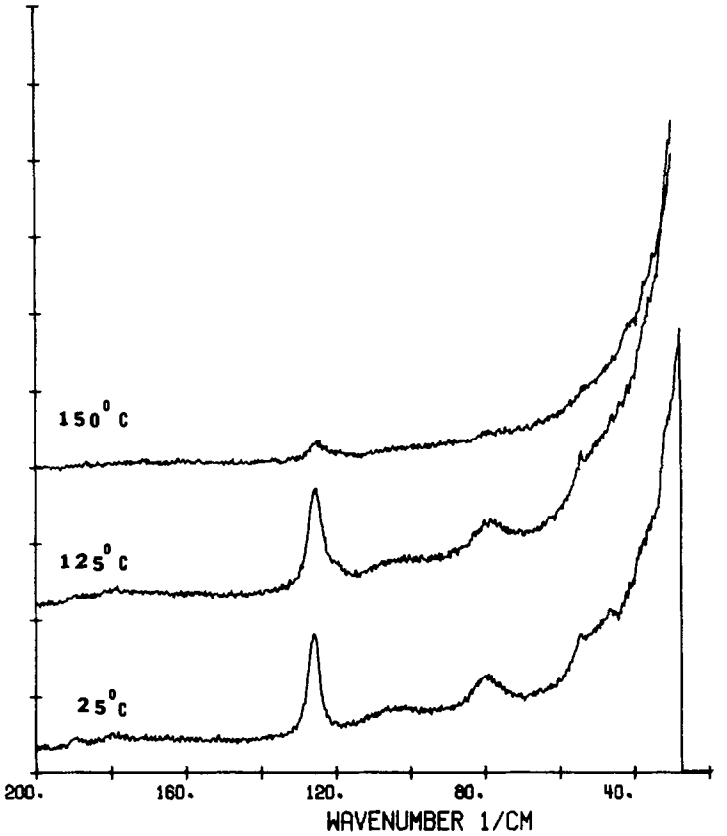

FIG. 2. Variable temperature Raman spectra of Ag_2ZnI_4.

solid solutions (*26*). Recent conductivity studies by Matsui and Wagner on the CuI–CdI_2 system indicate that increasing the concentration of CdI_2 lowers the temperature at which CuI undergoes its phase transition but raises the activation energies for ionic conduction (*27*). Our measurements are consistent with these results. All the other solid solutions were electronic conductors up to 250°C.

The gallium(I) ion is known to exist in its halide compounds (*28*); however, attempts to prepare Ga_2MX_4 (where M = Zn or Cd and X = Br or I) have failed. Different synthetic routes to these compounds are being explored. Similarly, the reaction of thallium iodide with several organic ammonium iodides in the solid state failed to produce any new compounds.

The reactions of organic ammonium iodides with indium(I) iodide are summarized in Table I. X-ray powder patterns show the presence of new phases in all of these reactions. The Raman spectra of all these new materials display a peak, usually quite strong, at 106–111 cm^{-1}, which can be assigned to In–I vibrations. However, the spectra of these materials are essentially unchanged up to 140°C. As seen in Table I, none of these tetraalkylammonium iodide–indium iodide systems shows significant ionic conductivity, the greatest being 5×10^{-5} $(ohm\text{-}cm)^{-1}$ for the methyl-pyridinium indium iodide (1 : 6.7) system.

Of the fairly large number of In and Tl halide systems which we have investigated the following were found to be good ionic conductors at elevated temperatures:

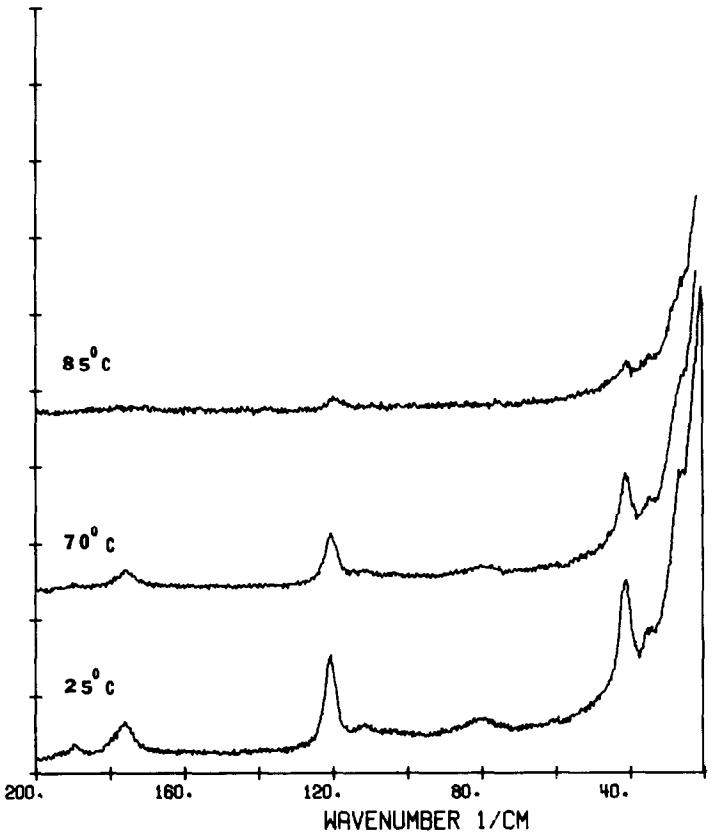

FIG. 3. Variable temperature Raman spectra of Ag_2CdI_4.

TABLE I

CONDUCTIVITIES OF INDIUM(I) IODIDE–ORGANIC AMMONIUM IODIDE DOUBLE SALTS

Organic Ammonium Iodide	Mole ratio of InI + organic ammonium iodide	Conductivity $(ohm\text{-}cm)^{-1}$ at 50°C
N,N'-dimethyltriethylenediammonium iodide	12:1	1×10^{-7}
Tetramethylammonium iodide	6.7:1	$<1\times10^{-10}$
Tetraethylammonium iodide	6.7:1	$<1\times10^{-10}$
N-methylpiperidinium iodide	6.7:1	$<1\times10^{-10}$
N-methylpyrrolidinium iodide	6.7:1	2×10^{-10}
Methylcyclohexylammonium iodide	6.7:1	6×10^{-7}
Methyldiethylcyclohexylammonium iodide	6.7:1	6×10^{-9}
N-methylpyridinium iodide	6.7:1	5×10^{-5}
N,N'-dimethylpiperazinium iodide	12:1	3×10^{-10}
Bis(triphenylphosphine)iminium iodide	6.7:1	2×10^{-9}

In_2ZnI_4, Tl_2ZnI_4, In_4CdI_6, and Tl_2ZnBr_4. As a representative member of this series, Tl_2ZnI_4 was chosen for single-crystal X-ray structure determination.

Structure of Tl_2ZnI_4

A single-crystal structure determination was performed on Tl_2ZnI_4 to determine the extent to which this material resembles the analogous silver ion conductor Ag_2HgI_4, for which detailed structural data are available (*29, 30*). The crystals of Tl_2ZnI_4 belong to the noncentric space group C_2^2–$P2_1$ with two formula units per cell. Important distances and angles are set out in Table II. The I sublattice consists of distorted close-packed I

TABLE II

DISTANCES (Å) AND ANGLES (deg) IN Tl_2ZnI_4

			Tl–I_u[a]		
Tl(1)–I(3)(65602)[b]		3.68(1)		Tl(2)–I(2)(65502)	3.61(1)
			Tl–I_t		
Tl(1)–I(1)(55601)		3.55(1)		Tl(2)–I(1)(55501)	3.57(1)
Tl(1)–I(4)(45601)		3.61(1)		Tl(2)–I(4)(55601)	3.58(1)
			Tl–I_b		
Tl(1)–I(1)(55602)		3.57(1)		Tl(2)–I(1)(65602)	3.49(1)
Tl(1)–I(2)(55601)		3.43(1)		Tl(2)–I(2)(65601)	3.51(2)
Tl(1)–I(3)(55601)		3.48(1)		Tl(2)–I(3)(55501)	3.54(1)
Tl(1)–I(4)(65602)		3.56(1)		Tl(2)–I(4)(65502)	3.49(1)
			Zn–I		
Zn–I(1)(65502)		2.63(2)		Zn–I(3)(55501)	2.61(2)
Zn–I(2)(55501)		2.57(2)		Zn–I(4)(55501)	2.64(2)
Tl(1)		Tl(2)		Tl(1)	Tl(2)
	I_b–Tl–I_b			I_b–Tl–I_u	
77.8(3)		78.9(3)		72.2(3)	73.6(3)
86.6(3)		89.7(3)		73.5(3)	74.0(3)
90.7(3)		90.7(3)		81.3(2)	85.4(3)
94.0(3)		94.3(3)		83.7(3)	87.5(3)
153.3(3)		159.4(3)			I_b–Tl–I_t
155.5(3)		160.2(3)		66.9(3)	67.4(3)
	I_t–Tl–I_t			69.5(3)	70.7(3)
86.2(3)		76.6(3)		76.6(3)	76.1(3)
	I_t–Tl–I_u			79.6(3)	78.4(3)
133.0(3)		136.1(3)		124.4(3)	115.2(3)
137.5(3)		140.6(3)		124.5(3)	115.7(3)
				129.0(3)	129.2(3)
				132.3(3)	132.3(3)
			I–Zn–I		
101.8(8)	108.6(7)	109.3(7)	110.8(8)	111.6(7)	114.0(8)

[a] The notation is

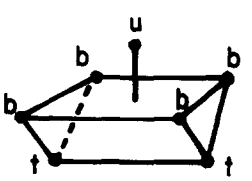

[b] The five-digit number denotes the iodine symmetry position as defined in Johnson's ORTEP program (ORNL-5138). Symmetry position 1 is x, y, z; symmetry position 2 is $\bar{x}, \frac{1}{2}+y, \bar{z}$.

layers, which are normal to the line of sight in the stereo view (Fig. 4). Within each layer there are threefold arrays of I, characteristic of closest packing, and square I arrays which are associated with nearby Tl ions. These layers are stacked in an A, B, C sequence. The Zn ions lie in tetrahedral sites between the layers with the Zn–I distance of 2.61 Å, and an average I–Zn–I angle of 109.4°. The two crystallographically independent Tl ions reside in sites of seven coordination (Fig. 5), which are associated with a threefold array of I in one layer and a fourfold array in the next. This I ligand environment closely approximates a C_{2v} capped trigonal prism, with Tl–I distances ranging from 3.43 to 3.68 Å. These capped trigonal prisms are stacked in columns parallel to the above-mentioned I layers, with the triangular faces shared between successive capped trigonal prisms in a column.

Seven coordination also can be discerned for Tl in the low-temperature form of TlI (*32*). However, in this case there is one very short distance, 3.36 Å to the capping I ion which compares with 3.6 Å in the present structure. The distance to each of the two I ions which lie on the edge opposite to the cap are long for TlI, 3.87 Å vs 3.6 for Tl_2ZnI_4. Even though the comparison between TlI and Tl_2ZnI_4 is facilitated by considering the Tl environment to be seven coordinate in both cases, the range of Tl–I distances in TlI led Helmholtz to describe the Tl environment as five-coordinate square pyramidal (*31*).

The seven coordination for Tl ions and the lack of a close-packed I array in Tl_2ZnI_4 contrasts with the four coordination of Ag and the approximate *ccp* array of I ions in Ag_2HgI_4. The dispositive ions, Zn and Hg, are found in tetrahedral coordination in both structures. Part of the difference between Ag and Tl in the two compounds undoubtedly stems from the larger size of the Tl ion. Tetrahedral coordination is common for the d^{10} silver ion which generally is found in nonpolar coordination geometries such as two-coordinate linear, three-coordinate planar triangular, and four-coordinate tetrahedral. The $d^{10}s^2$ thallous ion, like many post-transition metals of the same electronic configuration, often occurs in a polar coordination environment. The difference between d^{10} and $d^{10}s^2$ ions has been attributed by Orgel to the predominant contribution of the lowest excited state to the elctronic structure of the polarized ion (*32*). In the case of the d^{10} ions the lowest excited states are derived from d^9s^1, which has even orbital parity, and therefore these ions readily polarize to conform to nonpolar geometries such as the tetrahedron. The lowest excited states for $d^{10}s^2$ ions involve

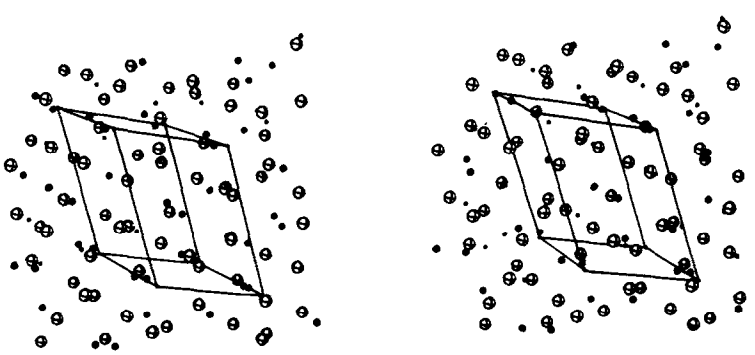

FIG. 4. Stereo view of Tl_2ZnI_4. The large spheres are I, the small black dots are Zn, and Tl is represented by intermediate-sized spheres. The close-packed layers of I are parallel to the plane of the paper.

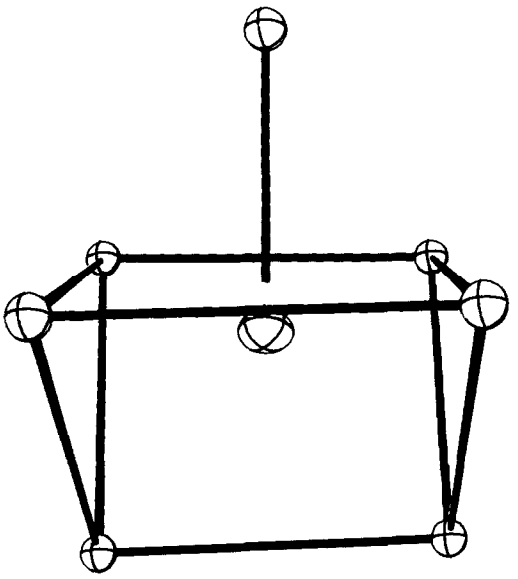

FIG. 5. Coordination polyhedron of Tl in Tl_2ZnI_4. This figure is representative of both Tl(1) and Tl(2).

the odd-parity configuration $d^{10}sp$, which promotes a polar coordination geometry, the capped trigonal prism being one of many such possibilities. A schematic representation of this argument is given in Fig. 6.

Inspection of the structure reveals some plausible conduction mechanisms for the Tl^+ ions. Adjacent to the occupied capped trigonal prism is a similar empty site which can become occupied by a translation of a Tl ion through a square face. This would open a vacancy on the formerly completely occupied trigonal pyramidal stack and provide a path up the stack for conduction. The bottleneck for conduction up this stack would be the passage through the triangular faces shared between the capped trigonal prisms. One unattractive feature of this proposal is that a close Tl-Tl contact would be necessary when a Tl passes near the displaced Tl. Another possible mechanism is that the Tl conduction might occur by partial occupation of the vacant tetrahedral sites by Tl. The obviously unattractive feature of this mechanism is the mismatch between the preferred high coordination number of Tl with the four coordination characteristic of a tetrahedral site. Further speculation on the conduction mechanism does not seem warranted before the structure of the high-temperature phase is determined.

Trends in Ion Transport

Table III summarizes conductivities in the disordered phase and activation energies for A_2MX_4 ionic conductors. The conductivities have been extrapolated where necessary to 150°C and are plotted in Fig. 7 along with the activation energies. Four general trends can be noted:

(1) The indium(I) and thallium(I) ionic conductors undergo the phase transition to the disordered phase at higher temperatures than the silver(I) and copper(I) conductors.

(2) The indium(I) and thallium(I) compounds are poorer ionic conductors than the silver(I) and thallium(I) conductors.

(3) The activation energies for ionic conduction are much greater for the indium(I) and thallium(I) compounds than for the silver(I) and copper(I) compounds.

(4) In addition, the present study of the alkylammonium halide derivatives shows that many types of compounds which are good Cu^+ or Ag^+ conductors do not have In^+ and Tl^+ ionic conducting analogues.

Thus the broad range of compounds which has been investigated consistently shows In^+ and Tl^+ to be less mobile than Cu^+ and Ag^+. There is a strong suggestion from the comparison of the Ag^+ and In^+ ions, which are of similar size, that decreased mobility is an inherent property of $d^{10}s^2$ ions. It is well known that structural factors are important in determining ionic mobility (*3*, *33*), and the present X-ray data on Tl_2ZnI_4 show that the structure of this compound is very different from that of Ag_2HgI_4 and Cu_2HgI_4. Even though we do not have structural data on the In compounds, it is common for In and Tl compounds to have similar structures, and therefore the difference between the d^{10} and $d^{10}s^2$ ions may simply result from differences

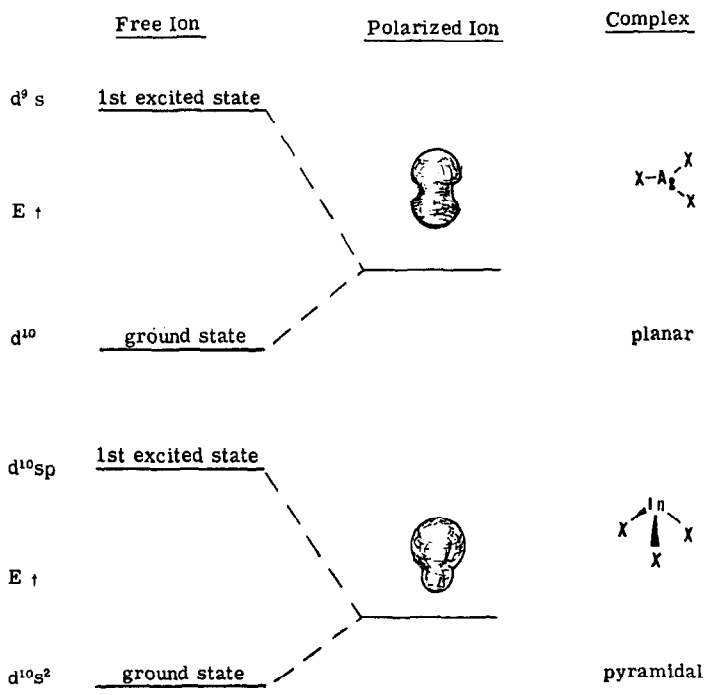

FIG. 6. Polarization of Ag^+ and In^+ by ligand fields.

TABLE III

CONDUCTIVITIES IN THE DISORDERED PHASE AND ACTIVATION ENERGIES FOR A_xMX_y IONIC CONDUCTORS

Compound	Temperature of phase transition (°C)	Total conductivity σ(ohm^{-1} cm^{-1}) at T (°C)	E_a (kJ mole^{-1})	Ref.
Ag_2HgI_4	50	10^{-3} at 60	36	*a*
Cu_2HgI_4	67	10^{-5} at 67	60	*b*
Cs_2HgI_4	245	10^{-6} at 250	79	*c*
Tl_2HgI_4	—	3×10^{-6} at 250	—	*d*
Ag_2ZnI_4	145	5×10^{-3} at 150	42	*c*
In_2ZnI_4	210	1.5×10^{-4} at 220	72	*c*
Tl_2ZnI_4	250	1.5×10^{-6} at 260	84	*c*
Ag_2CdI_4	80	7×10^{-3} at 100	41	*c*
In_4CdI_6	208	10^{-5} at 220	92	*c*
Tl_4CdI_6	—	6×10^{-9} at 50	—	*c*
In_2ZnBr_4	—	3×10^{-7} at 50	—	*c*
Tl_2ZnBr_4	212	3×10^{-6} at 220	99	*c*

[a] Reference (*4*).
[b] Reference (*5*).
[c] This work.
[d] G. Joy, Northwestern University, unpublished observations.

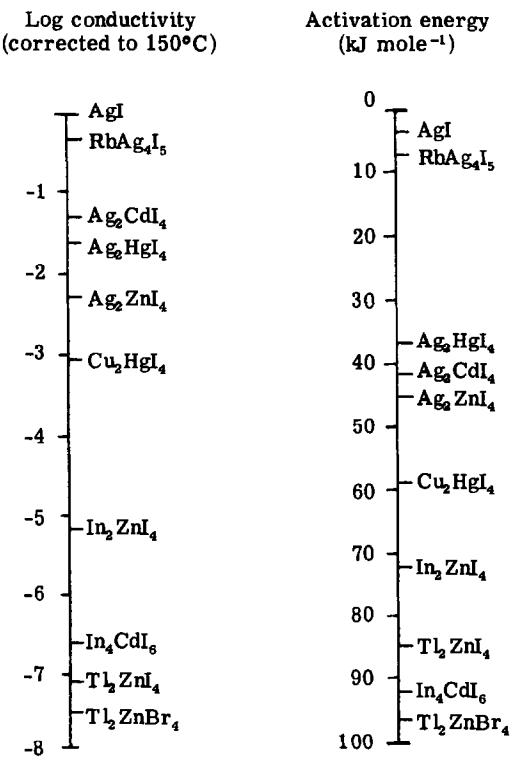

FIG. 7. Conductivities and activation energies of some ionic conductors.

in structure which in part are imposed by the different symmetry of the polarized ion.

There also is evidence for the polarizability to be important in the transition state for ion migration. One particularly clear example is the work of Sleight *et al.* on the isostructural series of compounds having the formula AM_2X_6 (A is Rb, Cs, or Tl; M is Ta, Nb, or W; X is O or F) the mobility of the Tl^+ ion is much greater than that of the Rb^+ ion (*12*). However, Tl^+ ion ($r = 1.54$ Å) is only slightly smaller than Rb^+ ion ($r = 1.58$ Å) (*13*). The great difference in their mobilities has been attributed to the fact that the Tl^+ ion is much more polarizable than the Rb^+ ion and can more readily change its shape to pass through the "bottleneck barrier." The ability of the Cu^+ and Ag^+ to adopt the necessary low coordination numbers has been attributed to their high polarizability, compared with alkali cations (*11*). However, just as the symmetry of the polarized ion may affect the crystal structure, it may also affect the energetics of the transition state. This argument is developed below.

The activation barrier in the heavy-metal halide conductors is thought to correspond to the mobile metal ion passing through the face of a halide polyhedron. In the case of Ag_2HgI_4 this would be the triangular face of a tetrahedron and for Tl_2ZnI_4 it might correspond to passage through a square or triangular face. In this model the potential energy maximum will occur when the ion is in a site of local D_{nh} symmetry, and thus in a nonpolar local environment. As already discussed above, the d^{10} Ag^+ and Cu^+ ions have readily accessible polarized configurations which are of even parity and therefore energetically favorable for the nonpolar bottleneck. By contrast, the $d^{10}s^2$ ions such as In^+ and Tl^+, for which the dipolar polarizability predominates, will not readily conform to the bottlenecks (Fig. 6).

For those ionic conductors in which the structures are known, the salts of d^{10} and $d^{10}s^2$ ions have different structures. Therefore we do not know the degree to which the difference in mobility between the d^{10} and $d^{10}s^2$ ions originates from simple structural differences rather than the ease of polarizing the ion in a symmetry which is compatible with the transition state. In this connection it should be pointed out that quadrupolar deformability of Ag^+ can explain unusual lattice dynamics and ion conductivity for silver halides (*34*, *35*).

Experimental Details

The congruently melting compounds were prepared from the melt by general procedures which have been described elsewhere (*17*). The incongruently melting silver and copper compounds and the organic ammonium iodide–metal iodide materials were prepared from appropriate quantities

of the component salts, which were mixed, compressed, and annealed in a sealed Pyrex vessel at elevated temperatures. The material was subsequently crushed, pressed, and heated several times to ensure equilibration. The equipment and techniques used for the Raman, DTA, and conductivity measurements have been described elsewhere (*17*).

Crystal Data

Initial experiments established that crystals of Tl_2ZnI_4, mounted in air, diffract X-rays for only a few hours before decomposing. Consequently, all samples were handled in an inert atmosphere box. The very large crystals, obtained as described above, had to be cut. The material is very soft, which made this cutting operation difficult and which probably resulted in the poor quality of the resultant cuttings.

On the basis of preliminary precession and Weissenberg photographs of crystal fragments sealed in glass capillaries, Tl_2ZnI_4 could be assigned to the monoclinic system. The only systematic absences noted, namely $0k0$ for k-odd, are consistent with space groups $P2_1$ and $P2_1/m$.

TABLE IV

SUMMARY OF CRYSTAL DATA, DATA COLLECTION, AND REFINEMENT

Compound	Tl_2ZnI_4
Formula weight	981.73 amu
a	7.661(9) Å
b	7.971(8) Å
c	10.074(13) Å
β	118.39(4)°
V	541.2 Å^3
Temperature	−160°C
Z	2
Density (calc)	6.02 g/cm^3
Space group	C_2^2–$P2_1$
Crystal dimensions	0.15 × 0.2 × 0.5 mm
Crystal shape	Approximated as bounding faces (012), (0$\bar{1}\bar{2}$), (0$\bar{1}$1), (01$\bar{1}$), (20$\bar{1}$), ($\bar{2}$01)
Crystal volume	0.016 mm^3
Radiation	Mo$K\alpha$ (λ(Mo$K\alpha_1$) = 0.70930 Å) from graphite monochromator
Linear absorption coefficient	434.7 cm^{-1}
Transmission factors	0.004 to 0.030
Takeoff angle	2.9°
Receiving aperture	6.5 × 6.5 mm, 32 cm from crystal
Scan method	Step scan in ω; 51 steps at 2 sec each from −2.0° in ω to +2.0° in ω
Background counts	10 sec each at ±2.25 in ω, with rescan option
2θ Limits	5.0 to 47.0°
Reflections scanned	$\pm h$, $\pm k$, $\pm l$
Total data observed	2972
p	0.04
Unique data ($P2_1$) having $F_o^2 > 3\,\sigma(F_o^2)$	689
Unique data ($P2_1/m$) having $F_o^2 > 3\,\sigma(F_o^2)$	486
Final number of variables	38
R	0.12
R_w	0.14
Error in observation of unit weight	2.66 electrons

For data collection a given crystal fragment was transferred under argon into the cold gas stream on the diffractometer. The inner nitrogen stream was at about −160°C and the outer nitrogen stream was at room temperature (*36*). The crystal, stuck with grease to the end of a glass rod, survived within these streams without further protection. Cell constants and other relevant data are given in Table IV.

Generally, ω-scans indicated considerable mosaicity in a given cutting. A number of cuttings were examined before one was found that gave satisfactory ω-scans. That cutting chosen for data collection was far from ideal, however. In addition to structure in ω, examination of reciprocal space revealed that the cutting consisted of two separate single but mosaic crystals, separated in orientation by about 10–15°. It was possible to center on one of these crystals, and in this way data were collected (*37*).

The data were processed in the usual way (*37*), using a value of p of 0.04. An attempt was made to correct for absorption effects, but this correction was necessarily approximate, owing to the irregular shape of the cutting and the very high linear absorption coefficient. After the absorption correction, the data were averaged assuming symmetry $2/m$. It was clear from this averaging process that the data were of very poor quality.

Solution and Refinement of the Structure

From the intensity distribution, hkl $h+l$ even strong and $h+l$ odd weak, we expected the Tl atoms to be approximately B centered in the cell. An origin-removed, sharpened Patterson map could not be interpreted on this basis in space group $P2_1/m$. Eventually, the data were scaled separately by parity class in the MULTAN78 system of programs and a solution was obtained in space group $P2_1$, based on 128 values of E. The seven highest peaks of the resultant E map satisfactorily yielded the structure.

Refinement proceeded along lines standard in this laboratory (*37*). Because the space group proved to be the polar one, $P2_1$, the data were reaveraged accordingly. However, in subsequent refinements it was clear that the structure is close enough to centrosymmetric so that $F(hkl)$ differs little from $F(\bar{h}\bar{k}\bar{l})$, especially when the errors in F_o are considered. Thus, the direction of the polar axis could not be established. Moreover, in view of the errors in the data we ultimately decided to average all four members of the form $\{hkl\}$, disregarding the polar nature of the group. The final refinement of 38 variables, based on 486 significant observations, converged to values of the conventional and weighted R indices of 0.12 and 0.14, respectively. An analysis of $\sum w(|F_o|-|F_c|)^2$ as a function of $|F_o|$, setting angles, and Miller indexes revealed no trends; the data are uniformly poor. The highest feature on a final difference Fourier map is 6.2 (1.4) e/Å^3, to be compared with a height of 57 e/Å^3 for the Zn ion on a previous Fourier map. Positional and thermal parameters are given in Table V.[1]

Acknowledgments

This research was supported by the Air Force Office of Scientific Research (Grant AFOSR 77-3227), and by the NSF MRL program through the Northwestern University Materials Research Center (Grant DMR 76-80847). We greatly appreciate stimulating discussions with Dr. P. Vashista, and the experimental assistance of Mark Honzel, who was supported by the NSF Undergraduate Research Program, in the preparation of alkyl- and arylammonium halide materials.

[1] A table of observed and calculated structure amplitudes has been deposited as No. 03451 for one page of supplementary material. Order from NAPS, c/o Microfiche Publications, P.O. Box 3513, Grand Central Station, New York, N.Y. 10017. Make checks payable to Microfiche Publications. Photocopies are $3.00 and Microfiche are $5.00. Outside the United States and Canada add $3.00 postage for photography or $1.00 for fiche.

TABLE V

POSITIONAL AND THERMAL PARAMETERS FOR Tl_2ZnI_4

Atom	x	y	z	B (Å^2)
Tl(1)	0.17253(94)[a]	0.51250[b]	0.94563(69)	3.2[c]
Tl(2)	0.68955(95)	0.52333(95)	0.43317(75)	3.2[c]
I(1)	0.2744(18)	0.2464(13)	0.2562(13)	1.68(21)
I(2)	0.2036(19)	0.4523(16)	−0.3801(12)	2.19(22)
I(3)	0.6785(17)	0.4447(15)	0.0832(12)	2.19(22)
I(4)	0.7625(18)	0.2356(13)	−0.2725(13)	1.66(20)
Zn	0.5789(31)	0.4725(24)	−0.2024(19)	1.85(36)

[a] Estimated standard deviations in the least significant figures are given in parentheses in this and all subsequent tables.

[b] Arbitrary origin.

[c] Equivalent isotropic thermal parameter. Tl(1) and Tl(2) were refined anisotropically according to the expression $\exp(-(\beta_{11}h^2+\beta_{22}k^2+\beta_{33}l^2+2\beta_{12}hk+2\beta_{13}hl+2\beta_{23}kl))$. The values of the β's for Tl(1) and Tl(2), respectively, are 0.0199(22), 0.0048(11), 0.0128(9), 0.0003(11), 0.0052(12), −0.0009(8) and 0.0183(22), 0.0069(13), 0.0135(10), 0.0019(11), 0.0063(12), −0.0004(8). The corresponding rms amplitudes of vibration are: Tl(1), 0.12(1), 0.21(1), 0.25(1); Tl(2), 0.14(1), 0.21(1), 0.24(1) Å.

References

1. C. A. TUBANDT AND E. LORENZ, *Z. Phys. Chem.* **87**, 513 (1914).
2. J. H. KENNEDY, *in* "Topics in Applied Physics," (S. GELLER, Ed.) Vol. 21, p. 105, Springer-Verlag, Berlin (1977).
3. K. FUNKE, *Progr. Solid. State Chem.* **11**, 345 (1976).
4. J. A. A. KETELAAR, *Z. Phys. Chem. Abt. B* **26**, 327 (1934).
5. L. SUCHOW AND G. POND, *J. Amer. Chem. Soc.* **75**, 5242 (1953).
6. J. N. BRADLEY AND P. D. GREENE, *Trans. Faraday Soc.* **63**, 424 (1967).
7. B. B. OWENS AND G. R. ARGUE, *Science* **157**, 308 (1967).
8. T. TAKAHASHI, *J. Appl. Electrochem.* **3**, 79 (1973).
9. D. O. RALEIGH, *J. Appl. Phys.* **41**, 1876 (1970).
10. K. H. LIESER, *Z. Phys. Chem.* **9**, 302 (1956).
11. R. D. ARMSTRONG, R. S. BOLMER, AND T. DICKINSON, *J. Solid State Chem.* **8**, 219 (1973).
12. A. W. SLEIGHT, J. E. GULLEY, AND T. BERGINS, *in* "Solid State Chemistry of Energy Conversion" (J. B. GOODENOUGH AND M. S. WHITTINGHAM, Eds)., p. 195, American Chemical Society, Washington, D.C. (1977).
13. F. A. COTTON AND G. WILKINSON, "Advanced Inorganic Chemistry," 3rd ed., p. 280, Interscience, New York (1972).
14. R. E. JONES AND D. H. TEMPLETON, *Acta Crystallogr.* **8**, 847 (1955).
15. P. L. GOGGIN AND I. J. MCCOLM, *J. Inorg. Nucl. Chem.* **28**, 2501 (1966).
16. G. CONTRERAS, J. S. POLAND, AND D. G. TUCK, *J. Chem. Soc. Dalton*, 922 (1973).
17. R. L. AMMLUNG, D. F. SHRIVER, M. KAMIMOTO, AND D. H. WHITMORE, *J. Solid State Chem.* **21**, 185 (1977).
18. D. F. SHIVER, G. JOY III, AND D. GREIG, *J. Electrochem. Soc.* **123**, 788 (1976).
19. C. O. QUICKSALL AND T. G. SPIRO, *Inorg. Chem.* **5**, 2232 (1966).
20. S. NAKASHIMA, H. YOSHIDA, T. FUKUMOTO, AND A. MITSUISHI, *J. Phys. Soc. Japan* **31**, 1847 (1971).
21. D. ROSS, I. W. SIDDIGI, AND H. J. V. TYRELL, *J. Chem. Soc. Dalton*, 1611 (1972).
22. V. I. MONASTRYSKAYA AND I. K. TOVMAS'YAN, *Issled. Termografi Korroz.*, 156 (1970).
23. P. H. FOURCROY, J. RIVET, AND J. FLAHAUT, *C. R. Acad. Sci. Paris* **278**, 1189 (1974).
24. Y. OTSUBO, A. NITTA, M. KANCKO, Y. IWATA, AND A. UEKI, *Kogyo Kagaku Zasshi* **69**, 1716 (1966).
25. D. R. GREIG, Ph.D. thesis, Northewstern University (1977).
26. G. HERRMANN, *Z. Anorg. Chem.* **71**, 296 (1911).
27. T. MATSUI AND J. B. WAGNER, JR., *J. Electrochem. Soc.* **124**, 937 (1977).

28. F. A. COTTON AND G. WILKINSON, "Advanced Inorganic Chemistry, 3rd ed., p. 280, Interscience, New York (1972).
29. K. W. BROWALL, J. S. KASPER, AND H. WIEDEMEIER, *J. Solid State Chem.* **10**, 20 (1974).
30. J. S. KASPER AND K. W. BROWALL, *J. Solid State Chem.* **13**, 49 (1975).
31. L. HELMHOLTZ, Z. KRIST., *A* **95**, 129 (1936)
32. L. E. ORGEL, "An Introduction to Transition-Metal Chemistry," p. 66, Wiley, New York (1960).
33. S. GELLER, *Accounts Chem. Res.* **11**, 87 (1978).
34. W. G. KLEPPMANN AND H. BLITZ, *Comm. Phys.* **1**, 105 (1976).
35. K. FISCHER, *Phys. Status Solidi.* **66**, 295 (1974).
36. J. C. HUFFMAN, Ph.D. thesis, Indiana University (1974).
37. See, for example, A. GLEIZES, J. REVELLI, AND J. A. IBERS, *J. Solid State Chem.* **17**, 363 (1976).